Theoretical Limit of $TiSi_2$ Contact Resistance

*Note: Sub-titles are not captured in Xplore and should not be used

M. Y. Jeong
CSE team, Innovation Center, Samsung Electronics
Hwaseong, Republic of Korea
my0808.jeong@samsung.com

M. A. Pourghaderi
CSE team, Innovation Center, Samsung Electronics
Hwaseong, Republic of Korea

K. Vuttivorakulchai
CSE team, Innovation Center, Samsung Electronics
Hwaseong, Republic of Korea

S. Song
CSE team, Innovation Center, Samsung Electronics
Hwaseong, Republic of Korea

Y.-S. Kim
CSE team, Innovation Center, Samsung Electronics
Hwaseong, Republic of Korea

M. Vörös
Device Laboratory Samsung Semiconductor Inc.
San Jose, California, USA

S. Jin
Device Laboratory Samsung Semiconductor Inc.
San Jose, California, USA

B. Lee
Device Laboratory Samsung Semiconductor Inc.
San Jose, California, USA

W. Choi
Device Laboratory Samsung Semiconductor Inc.
San Jose, California, USA

U. Kwon
CSE team, Innovation Center, Samsung Electronics
Hwaseong, Republic of Korea

D. S. Kim
CSE team, Innovation Center, Samsung Electronics
Hwaseong, Republic of Korea

***Abstract*—Improving contact resistance (R_{cnt}) becomes increasingly challenge in upcoming technology nodes. To figure out the fundamental limit of R_{cnt}, we employed the first-principles approach. DFT-NEGF analyses are performed considering the atomistic nature of dopant and necessary corrections for silicon band gap, as well as electronic correlation in metal. Our simulation setup successfully predicts the reported Schottky barrier height (SBH) and attainable R_{cnt} in Si/C49-$TiSi_2$ system.**

Keywords—Contact Resistance, Schottky Barrier Height, Density Functional Theory, Silicide

I. Introduction

In advanced nodes, silicide contact ought to be fitted within a few nanometer of foot print. To secure the contact area, high aspect ratio trenches with the chemical vapor deposition (CVD) metallization is commonly adopted. Realization of such a 3D profile with conformal coverage and minimal contamination is a delicate task. Besides these process complexities, the key challenge is the resistance value itself. The ambitious target for 3nm node is somewhere around $2\times10^{-9}-5\times10^{-9}$ Ω·cm2 [1]. In this study, the feasibility of such a target for $TiSi_2$ is investigated. To achieve such a low resistance, the tunneling-assistant mechanisms should be diligently co-optimized. The practical knobs to do so are the doping level and the silicide phase. The role of doping is simply to narrow down the barrier width, which in turn boosts the tunneling. However, the impact gets saturated around $5\times10^{20}-1\times10^{21}$ cm^{-3} dopant density [2]. To further decrease the resistance, Schottky barrier height (SBH) and defect distribution need be co-optimized. This is usually done through the careful control of the silicide phase and the consequent interface chemistry [3]. To estimate the achievable target of the contact resistance (R_{cnt}), given the involved chemistry of the problem, first-principles approach seems indispensable. Essentially, one needs to carefully account for the interfacial atomic configuration along with the corresponding electronic structure. Regarding the former, the model interface should present the thermodynamically sound sample for highly doped silicon in contact with the target silicide phase. As for the latter, density functional approximation should be tuned to give precise band gap and barrier height. Moreover, the energy and extent of interfacial states need to be accurate too. This is particularly challenging task for conventional density functional theory (DFT), as the system involves the localized d-state of transition metals [4].

In this study, we considered the practical level of doping [5] in pristine Si/C49-$TiSi_2$ system. The resulting non-equilibrium Green function (NEGF) combined with DFT (DFT-NEGF) setup can estimate the lowest limit of R_{cnt} for ideal process condition. The simulation steps are shown in Fig. 1. We prepared the structures and optimized by PBEsol. To compute the electronic structure, exchange-correlation functional is parameterized to reproduce the silicon gap. Then, Hubbard *U* correction is employed to adjust SBH and defect distribution. These settings are then exported to NEGF solver, where R_{cnt} is calculated using Landauer transmission formalism [6-8]. We found that the Hubbard *U*, extracted in *ab initio* manner, can adjust SBH to the experimental value and consequently corrects R_{cnt} by 10%. The impact of atomistic dopants on SBH and trap levels is also studied. Taking into account the DFT tuning and atomistic nature of dopants, our setup could reproduce the reported R_{cnt}.

II. Computational Details

We used linear combination of atomic orbital basis for all calculations. All the structures including atomistic doped configurations are relaxed by the PBEsol functional [9] to atomic force smaller than 20 meV/Å. For the PDOS and DFT-NEGF calculations, metaGGA functionals with DFT-1/2 corrections are used [10]. The DFT-1/2 parameters are optimized to reproduce the silicon bandgap and bandwidth. The 7×7×1 k-grids with density cutoff of 150 Hartree are applied for structure optimization and PDOS calculations.

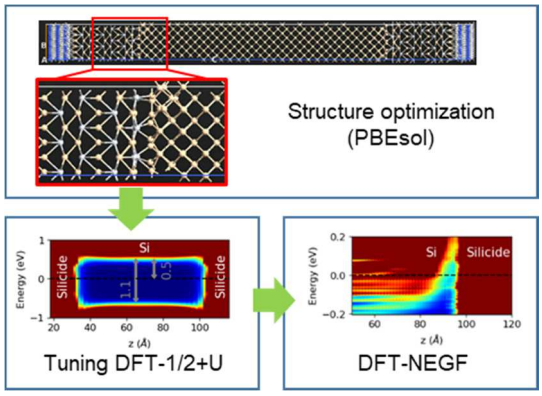

Fig. 1. The major steps to calculate R_{cnt} is demonstrated in this figure. Firstly, the model structures are relaxed with PBEsol functional. To study electronic properties, mGGA-1/2+U functional is carefully tuned. Finally, the structures are transformed to device setup to perform DFT-NEGF analysis.

The DFT-NEGF calculation are carried out with 13×13×1 k-mesh, while the transmission spectra are calculated with 51×51×1 k-mesh. The calculations in this report are performed with Quantum ATK [11] and the in-house tool.

III. Electronic Structure of Transition-Metal Silicide

The chemistry of the transition metals is mainly determined by the valance electrons in d-shell. In case of $TiSi_2$, the hybridization of Ti-*d* and Si-*p* makes the covalent backbone of the electronic structure. The density of state around the Fermi level can be roughly understood as combination of bonding, non-bonding and antibonding d-orbitals, as shown in Fig. 2. We verified our ligand field analysis by comparison the reference bulk and Si-vacant structures, as depicted in Fig. 3. In the case of Si/C49-$TiSi_2$ interface, Ti atoms tend to rearrange the interfacial silicon into configuration similar to bulk silicide. In other words, metal-rich interfaces try to convert the interfacial silicon into silicide configuration. However, the mere mismatch of the interface inflicts certain amount of missing bonds with extra non-bonding states. This scenario can be understood by benchmarking PDOS of titanium atoms deep in the metal against the ones located at the interface, Fig. 4. It has been already shown that these metal-dangling bonds (M_{DB}) are crucial for silicide contact. In fact, the weak Fermi level pinning and facet dependence of SBH are all signature of M_{DB} [12]. However, the accurate description of M_{DB}'s electronic structure is difficult for conventional DFT.

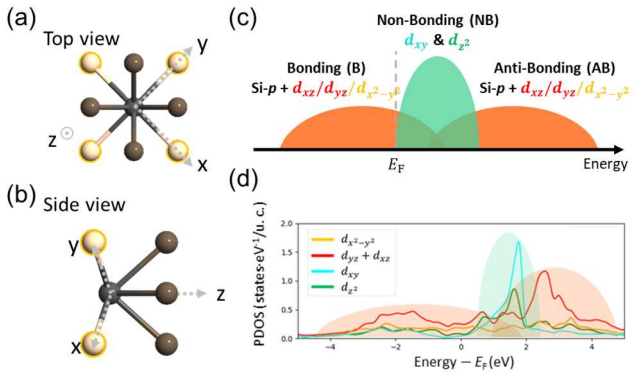

Fig. 2. Top and side view of C49 configuration are demonstrated in (a) and (b). The black, brown and beige spheres represent the Ti, out-of-plane Si and in-plane Si atoms, respectively. The schematic and calculated PDOS of the C49-TiSi2 are presented in (c) and (d).

In practice, popular exchange-correlation functionals tend to underestimate the Coulomb interaction of localized d-states, which in turn results in erroneous delocalization. The Hubbard U amendment is commonly applied as a low cost remedy. In this study, as shown in Fig. 5, the U parameter is calculated via linear response approach [13]. The estimated U, i.e. 3.7 eV, sets the correct energy for non-bonding states and fixes SBH very close to the experimental values [14]. In Fig. 6, the impact of U parameter on PDOS and effective charge transfer are illustrated. As expected, adding Hubbard term attenuates the charge transfer among titanium and silicon atoms, which effectively reduces SBH by ~40 meV.

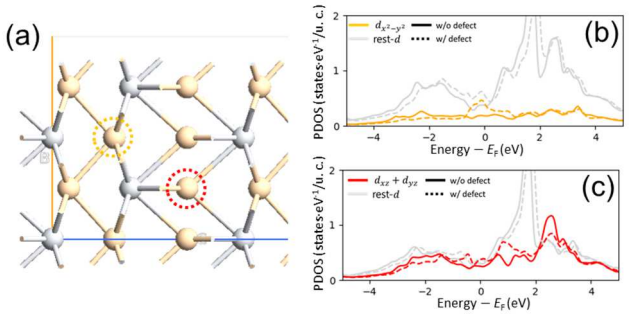

Fig. 3. To verify the ligand analysis in Fig. 2, two Si-Vacancy sites are studied, as shown in (a). The in-plane (out-of-plane) defect is marked with the orange (red) circle. In (b) and (c), PDOS of Ti w/ and w/o of Si-defects are presented. As expected, non-bonding peak appears in defective samples.

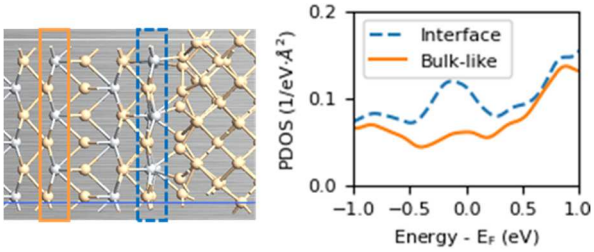

Fig. 4. PDOS of interfacial Ti is compared with bulk-like ones. The peak near the Fermi energy represents MDB states due to non-bonding *d*-orbitals.

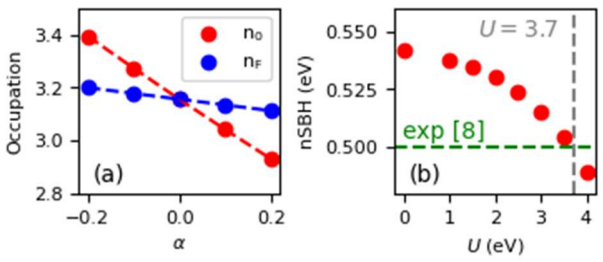

Fig. 5. (a) shows the d-occupations of a Ti atom to obtain Hubbard U parameter with linear response method. For our mGGA-1/2 setting, the Hubbard U value is ~3.7 eV. The sensitivity of nSBH to U parameters are shown in (b). The linear response U correctly predicts the experimental value.

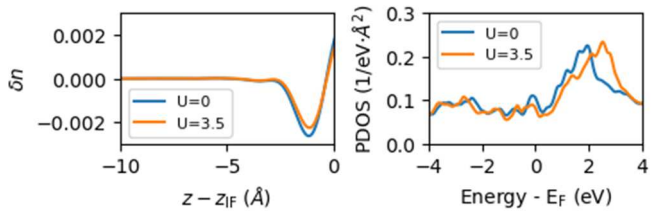

Fig. 6. The impact of U setting on differential density is shown in (a). The localization of M_{DB} hampers the charge transfer. In (b), the corresponding correction on PDOS for interfacial $TiSi_2$ is illustrated.

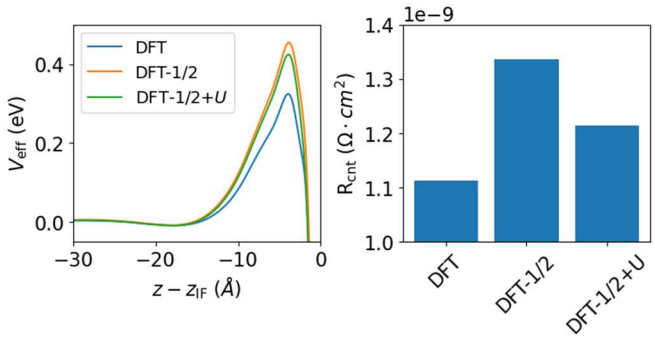

Fig. 7. (a) shows the influence of DFT-1/2 and + U (U=3.7 eV) correction in effective potential for DFT-NEGF calculations. The resulted R_{cnt} values are presented in (b). The SBH and R_{cnt} increase (decrease) by DFT-1/2 correction (+U correction).

Following the steps in Fig. 1, Hubbard U and DFT-1/2 setting are exported to device simulator. The subsequent impact of functional tuning is shown in Fig. 7. As expected, DFT-1/2 treatment widens the Silicon gap, which results in larger SBH and thicker barrier. Consequently, the resistance increases by ~20%. However, adding U correction lowers SBH, as shown in Fig. 5, and brings ~10% reduction in resistance.

IV. Atomistic Presentation of Doped Silicon

For precise modeling of SBH, the impact of image charge is crucial [15]. The atomic representation of dopants near the metallic interface guarantees the accurate dipole interactions. In this report, a pool of 36 interface samples is prepared, which covers all possible phosphorus substitutions corresponding to 7.3×10^{20} cm^{-3} density. To be consistent with the actual silicidation process [3], the domain of doping is extended into the metallic layer. All structures are prepared in periodic boundary condition with 8nm of silicon slab. The relaxation and energetic estimation are carried out by PBEsol functional. In the next step, the equilibrium partition function is used as the weighting factor, as shown in Fig. 8. The lowest energy sample has phosphorous inside silicon, whilst the second important one allocates dopant in metal layer. The weighting factor is negligible for the rest of the samples.

Eventually, the important model structures are transformed to device architectures for DFT-NEGF analysis as shown in Fig. 9. To understand the impact of phosphorous dopant, the interfacial $TiSi_2$ PDOS and position dependent effective potential are compared with the case of homogenous background doping (HBD). As shown in Fig. 10, consideration of ion can changes the PDOS and SBH. For important samples we calculated, the phosphorus dopant reduces M_{DB} and increases the SBH. The raise of barrier height combined with ionized impurity scattering and reduced PDOS near Fermi level escalates R_{cnt} by 10%, as depicted in Fig. 11. Especially, the shape of the transmission seems to have strong correlation between the shape of PDOS. This implies the M_{DB} influenced by Hubbard U and ionic dopant is an important factor which determines R_{cnt}.

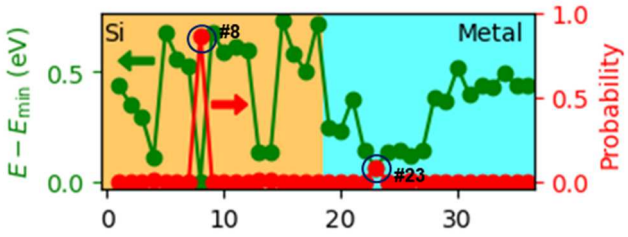

Fig. 8. The energy difference and the related probability function are shown for atomically doped structures. For the first 18th samples, phosphorous are contained in silicon. For the rest of samples, dopant diffused into metal.

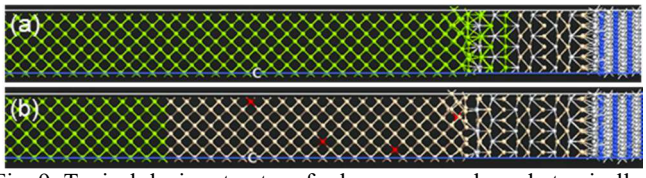

Fig. 9. Typical device structure for homogeneously and atomically doped samples are shown in (a) and (b). The blue, white, beige, green and red spheres represent N, Ti, Si, n-doped Si, and P, respectively.

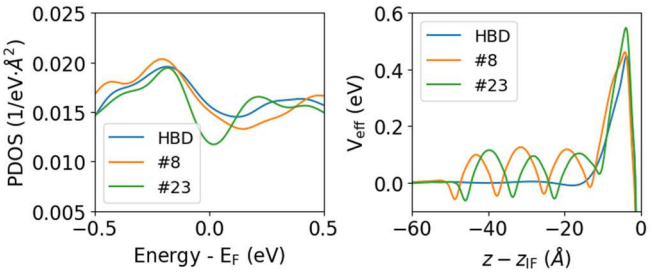

Fig. 10. The left panel shows the PDOS of interfacial $TiSi_2$ with doped Si/$TiSi_2$ interface calculated via DFT-1/2+U (U=3.7 eV). The M_{DB} states strongly affected by the atomistic dopant. The effective potential is benchmarked between HBD and sample #8 and #23 in Fig. 8 (right panel). The atomically doped sample gives higher SBH.

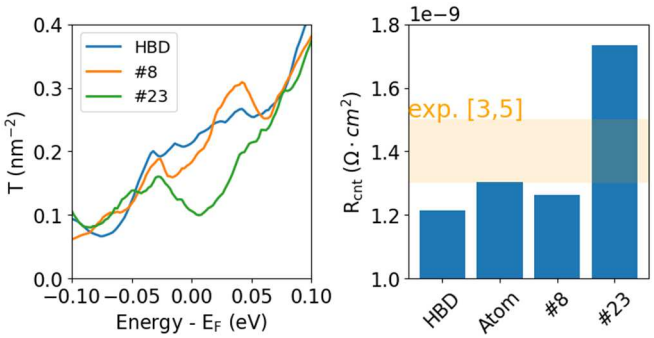

Fig. 11. In left panel, Landauer transmission are shown for important samples. The corresponding R_{cnt} are depicted in right panel. In effect, atomic doping increases the R_{cnt} by 10% to the limiting value of 1.3×10^{-9} $\Omega\cdot cm^2$. The shaded area demonstrates the experimental Rcnt corresponds to active doping N_D=7-9×10^{20} cm^{-3} [3, 5].

V. Conclusion

The DFT description of $TiSi_2$ is improved by Hubbard model. The *U* parameter is extracted in *ab initio* way. This setting successfully predicts SBH and trap distribution of Si/C49-$TiSi_2$ interfaces. Considering the impact of dopant ions, the transport simulation predicts 1.3×10^{-9} $\Omega\cdot cm^2$ as the theoretical limit of R_{cnt} for 7.3×10^{20} cm^{-3} doping density, which is close to measurement [3].

Acknowledgment

The authors would like to thank Søren Smidstrup and Yongju Kang from SYNOPSYS for their technical supports.

References

[1] P. Raghavan et al., "Holisitic device exploration for 7nm node" 2015 IEEE CICC 1-5 (2015)

[2] Z. N. Weinrich et al., "Dopant-defect interactions in highly doped epitaxial Si:P thin films" Thin Solid Films, **685**, 1 (2019)

[3] H. Yu et al., "Titanium Silicide on Si:P With Precontact Amorphization Implantation Treatment: Contact Resistivity Approaching 1×10^{-9} Ohm-cm^2" IEEE Transactions on Electron Devices, **63**, 12 (2016)

[4] V. I. Anisimov, J. Zaanen, and O. K. Andersen, "Band theory and Mott insulators: Hubbard *U* instead of Stoner *I*" PRB, **44**, 943 (1991)

[5] H. Yu et al., "Lanthanum and Lanthanum Silicide Contacts on N-Type Silicon" IEEE Electron Device Letters, **38**, 7 (2017)

[6] J. Maassen, C. Jeong, A. Baraskar, M. Rodwell, M. Lundstrom, "Full band calculations of the intrinsic lower limit of contact resistivity" Appl. Phys. Lett., **102**, 111605 (2013)

[7] T. Markussen and K. Stokbro "Metal-InGaAs contact resistance calculations from first principles" 2016 International Conference on Simulation of Semiconductor Processes and Devices (SISPAD), 373 (2016)

[8] K. Vuttivorakulchai et al., "Surface scattering impact on Si/TiSi2 contact resistance" Solid State Electronics **201**, 108583 (2023)

[9] J. P. Perdew et al., "Restoring the Density-Gradient Expansion for Exchange in Solids and Surfaces" Phys. Rev. Lett., **100**, 136406 (2008)

[10] L. G. Ferreira, M. Marques, and L. K. Teles, "Approximation to density functional theory for the calculation of band gaps of semiconductors" Phys. Rev. B, **78**, 125116 (2008)

[11] S. Smidstrup et al., "QuantumATK: an integrated platform of electronic and atomic-scale modelling tools" J. Phys. Condens. Matter **32**, 015901 (2019)

[12] L. Lin, Y. Guo and J. Robertson, "Metal silicide Schottky barriers on Si and Ge show weaker Fermi level pinning" Appl. Phys. Lett., **101**, 052110 (2012)

[13] M. Cococcioni, and S. de Gironcoli, "Linear response approach to the calculation of the effective interaction parameters in the LDA+U method" PRB, **71**, 035105 (2005)

[14] S. Mao, and J. Ruo, "Titanium-based ohmic contacts in advanced CMOS technology" J. Phys. D: Appl. Phys. **52**, 503001 (2019)

[15] Y. Nishi et al., "Schottky barrier height modulation by atomic dipoles at the silicide/silicon interface" PRB, **84**, 115323 (2011)